JASS Journal of Astronomy and Space Sciences

GPS TEC Fluctuations in the Low and High Latitudes During the 2015 St. Patrick's Day Storm

Jong-Kyun Chung[1][†], Junseok Hong[1, 2], Sung-Moon Yoo[1], Jeong-Han Kim[3], Geonhwa Jee[3], Valery V. Hegai[4]

[1]Korea Astronomy & Space Science Institute, Daejeon 34055, Korea
[2]Department of Astronomy, Space Science and Geology, Chungnam National University, Daejeon 34134, Korea
[3]Korea Polar Research Institute, Incheon 21990, Korea
[4]Pushkov Institute of Terrestrial Magnetism, Ionosphere and Radiowave Propagation, Russian Academy of Sciences (IZMIRAN), Moscow, Troitsk 142190, Russia

As a part of collaborative efforts to understand ionospheric irregularities, the Korea ionospheric scintillation sites (KISS) network has been built based on global positioning system (GPS) receivers with sampling rates higher than 1 Hz. We produce the rate of TEC index (ROTI) to represent GPS TEC fluctuations related to ionospheric irregularities. In the KISS network, two ground-based GPS sites at Kiruna (marker: KIRN; geographic: 67.9° N, 21.4° E; geomagnetic: 65.2° N) and Chuuk (marker: CHUK; geographic: 7.5° N, 151.9° E; geomagnetic: 0.4° N) were selected to evaluate the ROTI value for ionospheric irregularities during the occurrence of the 2015 St. Patrick's Day storm. The KIRN ROTI values in the aurora region appear to be generally much higher than the CHUK ROTI values in the EIA region. The CHUK ROTI values increased to ~0.5 TECU/min around UT=13:00 (LT=23:00) on March 16 in the quiet geomagnetic condition. On March 17, 2015, CHUK ROTI values more than 1.0 TECU/min were measured between UT=9:00 and 12:00 (LT=19:00 and 22:00) during the first main phase of the St. Patrick's Day storm. This may be due to ionospheric irregularities by increased pre-reversal enhancement (PRE) after sunset during the geomagnetic storm. Post-midnight, the CHUK ROTI showed two peaks of ~0.5 TECU/min and ~0.3 TECU/min near UT=15:00 (LT=01:00) and UT=18:00 (LT=04:00) at the second main phase. The KIRN site showed significant peaks of ROTI around geomagnetic latitude=63.3° N and MLT=15:40 on the same day. These can be explained by enhanced ionospheric irregularities in the auroral oval at the maximum of AE index

Keywords: GPS TEC fluctuation, rate of TEC index, ionospheric irregularity, low and high latitudes

1. INTRODUCTION

It is well known that the radio signals (L1=1.57542 GHz and L2=1.22760 GHz) of global positioning system (GPS) satellites propagating through the ionosphere undergo rapid variations of amplitude and phase, referred to as scintillations, which are caused by ionospheric irregularities (Aarons 1997; Pi et al. 1997; Kintner et al. 2007; Li et al. 2010a). Ionospheric irregularities can be observed through GPS total electron content (TEC) fluctuations, which could be hazard in terms of the continuity and availability of GPS performance parameters (Cherniak et al. 2014; Bang et al.

2016). Availability is the percentage of time that services are usable by the navigator and continuity is the probability that GPS performance is maintained for the duration of operation. All satellite navigation systems have specific requirements of availability and continuity during their operation phase (Langley 1999). Therefore, measurements of GPS TEC fluctuations are especially important to monitor the operation performances of satellite navigation systems in the low and high latitudes where severe ionospheric irregularities mainly occur (Skone 2001; Jacobsen & Dähnn 2014; Jacobsen & Andalsvik 2016).

In low latitudes, ionospheric irregularities are known

to occur frequently in the equatorial ionospheric anomaly (EIA) region, which has the largest gradients of electron density in the Earth. Intense ionospheric scintillation has been predominantly measured in the EIA crests, which are located approximately 15° north and south latitudes of the magnetic equator (Aarons, 1982; Chu et al. 2008; Muella et al. 2008; Deng et al. 2013; Abadi et al. 2014; Magdaleno et al. 2017). The EIA crests are formed during the daytime when thermospheric winds generate the eastward dynamo electric field. The electric field ($\vec{E}$) perpendicular to the magnetic field ($\vec{B}$) at the magnetic equator drives the upward plasma drift ($\vec{E} \times \vec{B}$), which invariably falls down along magnetic field lines to higher latitudes under gravity and pressure gradients. The electron density finally reaches the maximum in two bands at ~15° north and south latitudes called the EIA crests. Their shapes may not be symmetrical in the northern and southern hemispheres due to thermospheric winds. During the nighttime, the enhanced electron density in the EIA crests can be sustained depending on the recombination rate between electrons and neutral components with varying altitudes, and equatorial ionospheric bubbles of plasma depletion can occur after sunset. When the bubbles, which are initiated in the magnetic equator, move to the EIA crests, they can produce intense ionospheric irregularities in the EIA crests with high electron density. As a result, strong GPS TEC fluctuations may occur in the EIA crests at nighttime (Abadi et al. 2015; Jiao & Morton 2015).

In high-latitudes, ionospheric irregularities have been often measured in polar cap patches and the boundary of the auroral oval (Cherniak et al. 2014, 2015). Polar cap patches with horizontal sizes from 100 to 1,000 km are localized enhancement blobs with electron densities of 2-20 times larger than background ionosphere at altitudes of the F-region (Kintner et al. 2007). These patches are known to be generated at the dayside cusp region, and then rapidly move with a polar background convection velocity of ~500 m/s towards midnight. Ionospheric irregularities associated with polar cap patches can also cause GPS TEC fluctuations in the F-region due to their steep gradients of electron densities. In addition to polar cap patches, GPS TEC fluctuations can be generated by electron precipitation with energies ranging from eV to tens of keV. Electron precipitation with lower energies can produce ionization in the F-region, and those with higher energies can produce ionization in the E-region. Both the E- and F-regions can produce GPS TEC fluctuations. Basu et al. (1983) and Kintner et al. (2002) reported GPS TEC fluctuations originating from the E-region.

The event of the St. Patrick's Day storm on March 17–18, 2015 was investigated to evaluate the first results of GPS TEC fluctuations from the Korea ionospheric scintillation sites

(KISS) network, which is the collaborative effort between the Korea Astronomy & Space Science Institute (KASI) and Korea Polar Research Institute (KOPRI). In Section 2, we briefly introduce the KISS network and the data processing method for the GPS TEC fluctuation. The results from the first KISS network campaign are described in Section 3. Finally, we summarize the test results and further works of the KISS network.

2. MEASUREMENTS

2.1 Korea Ionospheric Scintillation Sites (KISS) Network

To understand ionospheric climatology and its global dynamical responses to geomagnetic and atmospheric disturbances, KASI and KOPRI built the KISS network, which is based on high-rate GPS receivers with a measurement time of less than 1 sec and software to compute GPS measurement parameters for ionospheric irregularities. Table 1 shows the regional characteristics of each GPS site of the KISS network in 2107. As shown in Table 1, the connected autonomous space environment sensor (CASES) system is the specific designed GPS receiver system for ionospheric measurements. The CASES receivers, which have been operating at Kiruna (KIRN) and Ny-Ålesund (NYSD) in the Arctic and King Sejong (KSJ2) and Jangbogo (JBG2) stations in the Antarctic, have constantly measured GPS TEC from different ionospheric time delays between GPS L1 and L2 signals with a sampling rate of 1 Hz (1 sample/s). In addition, they can automatically capture the phase and amplitude distortions of L1 and L2 signals at a sampling rate of 100 Hz (100 samples/s) if ionospheric irregularities are detected. Detailed technical information of the CASES system and its data processing algorithms can be found in the works of O'Hanlon et al. (2011) and Deshpande et al. (2012). The receivers at classical geodetic GPS sites Chuuk (CHUK), Jeju (JEJU), Daejeon (DAEJ), and Sainshand (SHND) have been operating at a sampling rate of 1 Hz. GPS TEC data with a temporal resolution of one second are commonly used for measurements of GPS TEC fluctuations caused by ionospheric irregularities (Jacobsen & Dähnn 2014; Cherniak et al. 2015).

In this work, we selected two sites, KIRN (geographic: Lat=67.9° N, Lon=21.4° E; geomagnetic: Lat=65.2° N) and CHUK (geographic: Lat=7.5° N, Lon=151.9° E; geomagnetic: Lat=0.5° N), in the northern high and low latitudes, respectively. The two GPS sites in the KISS network are located in the aurora and EIA regions, and could evaluate ionospheric irregularities with the measurement of GPS TEC fluctuations at a temporal resolution

Table 1. List of GPS sites in the KISS (Korea Ionospheric Scintillation Sites) network

Site	City, Country Geographic Location	Ionospheric Region Geomagnetic location	Target	Start Year	Agency
CHUK	Chuuk, Micronesia Lat=7.5° N, Lon=151.9° E	EIA Trough Lat=0.4° N, Lon=136.0° E, I=0.7°	Geodesy	2011.10.15	KASI
JEJU	JEJU, Korea Lat=33.2° N, Lon=126.7° E	Mid-latitude Lat=23.8° N, Lon=162.3° E, I=48.9°	Geodesy	2000.06.22	KASI
DAEJ	Daejeon, Korea Lat=36.4° N, Lon=127.4° E	Mid-latitude Lat=27.1° N, Lon=198.1° E, I=53.0°	Geodesy	1999.03.19	KASI
SHND	Sainshand, Mongolia Lat=44.9° N, Lon=110.1° E	Mid-latitude Lat=35.0° N, Lon=182.4° E, I=65.2°	Geodesy	2011.08.29	KASI
KIRN	Kiruna, Sweden Lat=67.9° N, Lon=21.4° E	Auroral oval Lat=65.2° N, Lon=127.3° E, I=77.5°	Ionosphere	2014.09.24	KOPRI
NYSD	Ny-Ålesund, Norway Lat=78.9° N, Lon=11.9° E	Polar Cap Lat=76.0° N, Lon=115.7° E, I=82.6°	Ionosphere	2015.10.10	KOPRI
KSJ2	King Sejong Station, Antarctic Lat=62.2° S, Lon=301.2° E	Weddell Sea Anomaly Lat=52.6° S, Lon=10.6° E, I=-55.6°	Ionosphere	2015.03.01	KOPRI
JBG2	Jangbogo Station, Antarctic Lat=74.6° S, Lon=164.2° E	Auroral Oval/Polar Cap Lat=77.0° S, Lon=274.4° E, I=-82.4°	Ionosphere	2016.12.01	KASI

of one second during the occurrence of the St. Patrick's Day storm.

2.2 Rate of TEC Index

In this study, ionospheric irregularities are described by the rate of TEC Index (ROTI) of the GPS TEC fluctuations. It is closely related with GPS scintillation caused by ionospheric irregularities (Jacobsen & Dähnn, 2014). GPS ROTI can be calculated using dual-frequency GPS receiver measurements with sampling at 1 Hz, which are much more widely distributed compared to scintillation GPS receivers with sampling at 50 or 100 Hz. Pi et al. (1997) proposed the ROTI of the standard deviation of the Rate of TEC (ROT) with a running window of 5 min as shown in Equations (1) and (2).

$$ROT = \frac{TEC_k^i - TEC_{k-1}^i}{(t_k - t_{k-1})} \qquad (1)$$

$$ROTI = \sqrt{\langle ROT^2 \rangle - \langle ROT \rangle^2} \qquad (2)$$

where TEC represents slant TEC (STEC), i is a visible GPS satellite, and t_k is the time of epoch. GPS receiver independent exchange format (RINEX) data were sampled at intervals of 1 second. ROT and ROTI are calculated in units of TECU/min (1 TECU = 10^{16} electrons/m²) for each satellite over GPS sites for a cutoff elevation angle over 30° to minimize the multipath effect. The multipath effect is a range delay error where GPS signals transmitted from the satellite reaches the GPS antenna after one or more paths due to water reflection, terrestrial structures, and other objects. The location of each ROTI value is the ionospheric pierce point (IPP) of the intersection of the receiver-to-satellite line with the thin shell ionosphere. The IPP height was assumed to be 350 km in this work. Fig. 1 shows variations in ROTI values measured at
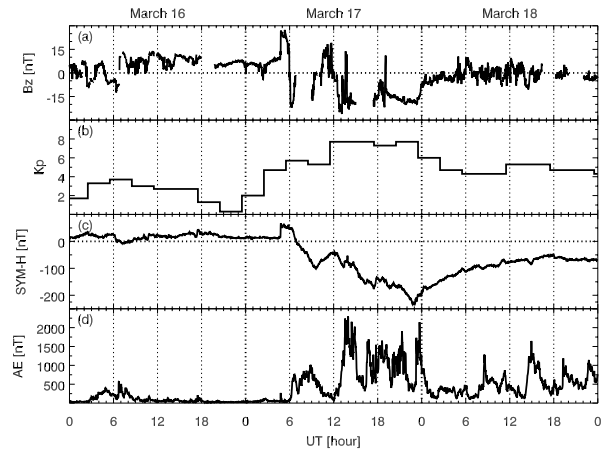
Fig. 1. Geomagnetic variations between March 16 and 18, 2015.

Kiruna and Chuuk between March 16 and 18, 2015.

2.3 The 2015 St. Patrick's Day Storm

Fig. 2 shows variations in the interplanetary magnetic field (IMF) and geomagnetic activity indices between March 16 and 18, 2015. In Fig. 2(a), the IMF B_z component appears to be approximately 25 nT at the sudden storm commencement (SSC), sharply turn southward at UT=05:30, and alternates its directions between north and south on March 17. The Kp index (Fig. 2(b)) of the magnitude of geomagnetic storm reached a value of 8 after UT=12:00 on March 17. The SYM-H index showed that the SSC occurred at UT=04:45, and the main phase lasted for 16 hr between UT=07:00 and UT=23:00 with a minimum of -226 nT on March 17; the recovery phase occurred on March 18 (Fig. 2(c)). The auroral electrojet (AE) index revealed wide variations on March 17 and 18. The strong geomagnetic disturbances on March 17 and 18, 2015 led to ionospheric irregularities through coupling among the
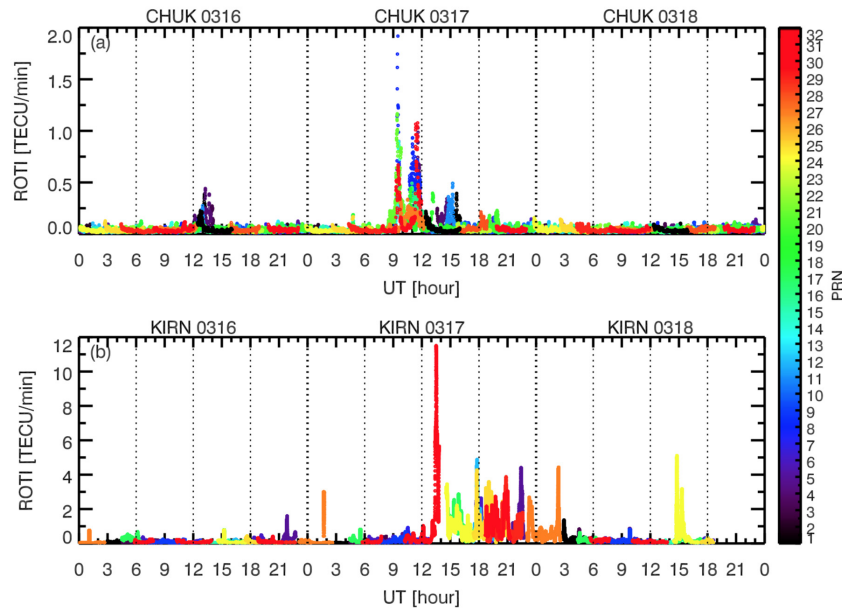
Fig. 2. GPS ROTI variations measured at CHUK (geographic: 7.5° N, 151.9° E; geomagnetic: 0.4° N) and KIRN (geographic: 67.9° N, 21.4° E; geomagnetic: 65.2° N) between March 16 and 18, 2015.

ionosphere-thermosphere-magnetosphere in the polar and equator regions.

3. RESULTS AND DISCUSSION

In these studies, rapid GPS TEC fluctuations were examined using ROTI, which is defined as the standard deviation taken over 5 min of the rate of change of GPS TEC sampled at 1 Hz. We determined ROTI values to detect ionospheric irregularity features at the KIRN and CHUK sites, which are located in the aurora and EIA regions, respectively. Fig. 2 shows temporal variations of ROTI values to be calculated using GPS STEC, which was obtained from all visible pseudo-range noise (PRN) GPS satellites over the elevation angle of 30° at the KIRN and CHUK sites from March 16 to 18. The PRN acts as an identification number for each GPS satellite.

KIRN ROTI values in the aurora region were generally much higher than those at the CHUK site in the EIA trough. This is not consistent with the results that GPS scintillation in the equatorial region is generally more severe than that in high latitude (Jiao & Morton 2015). They reported the characteristics of high latitude and equatorial scintillation using commercial ionospheric scintillation GPS receivers (Novatel GSV4004V and Septentrio PolarRxS), which are in operation in Alaska, Jicamarca, and Ascension Island. Li et al. (2010b) showed differences in the longitudinal occurrences of equator ionospheric irregularities due to the combined effects of the prompt penetration of eastward

electric field (PPEF), disturbance dynamo electric field (DDEF), and gravity waves. Therefore, differences in ROTI between KIRN and CHUK may be relatively higher than those between Alaska and Jicamarca/Ascension Island due to the longitudinal location. Another reason for higher KIRN ROTI than CHUK ROTI is that GPS ROTI may reflect more phase scintillation rather than amplitude scintillation. Jiao & Morton (2015) reported that phase scintillation is more severe than amplitude scintillation in the high latitude compared with lower latitudes using GPS scintillation parameters (S_4 and σ_ϕ indices), which are estimated from GPS signal intensity and carrier phase measurements.

As shown in Fig. 3(a), the CHUK ROTI values increased to ~0.5 TECU/min and ~1.1 TECU/min around UT=13:00 (LT=23:00) on March 16 and UT=11:30 (LT=21:30) on March 17, respectively. Chung et al. (2016) analyzed the seasonal and local time variations of CHUK GPS TEC. They presented frequent observations of an unusual enhancement in GPS TEC around LT=22:00 during spring. This abnormal GPS TEC increase may lead to high ROTI values. Most CHUK ROTI values more than 1.0 TECU/min were distributed at UT=09:30 (LT=19:30). Jiao & Morton (2015) reported that occurrences of equatorial ionospheric scintillations are mostly distributed between one and two hours after sunset at Jicamarca and Ascension Island. This may be due to ionospheric irregularity by pre-reversal enhancement (PRE) leading to an enhanced upward $\vec{E}\times\vec{B}$ drift post-sunset (Abadi et al. 2015). On March 17 post-midnight, ROTI showed two peaks of ~0.5 TECU/min and ~0.3 TECU/min near UT=15:00

(LT=01:00) and UT=18:00 (LT=04:00) at the second main phase and Kp=8.

Fig. 2(b) shows that variations of KIRN ROTI are similar to the AE index variations in Fig. 1(d). The peak of ROTI was detected at the KIRN GPS ionospheric site at geomagnetic latitude=63.3° and MLT=15:40 on March 17, 2015. The geomagnetic latitude and magnetic local time (MLT) are the IPP location and time of the ROTI measurement calculated using the STEC value. Cherniak & Zakharenkova (2016) analyzed ionospheric irregularities at high latitudes during the period of the 2015 St. Patrick's Day storm using 2-D ROTI maps from ground-based GPS sites and Swarm, GRACE, and TerraSAR-X satellites in a near polar orbit at altitudes of 450–500 km. They found that intense ionospheric irregularities occur in the auroral oval within 60°–70° MLAT between 15:00 MLT and 17:00 MLT in the northern hemisphere, and revealed that the strongest ionospheric irregularities related to the polar tongue of ionization (TOI) appear in the day-night side across the polar cap. Considering the measurement time and location, the maximum value of the KIRN ROTI value in Fig. 2(b) may be attributed to strong ionospheric irregularities in the auroral oval and not the TOI.

4. SUMMARY AND CONCLUSIONS

We present the first results of GPS TEC fluctuations during the period of the 2015 St. Patrick's Day storm using the KISS network, which is the collaborative effort between the KASI and KOPRI to understand ionospheric irregularities and their effects on GPS radio signals. We calculated the ROTI values using 1 Hz measurements of two ground-based GPS sites at Kiruna (geographic: 67.9° N, 21.4° E; geomagnetic: 65.2° N) and Chuuk (geographic: 7.5° N, 151.9° E; geomagnetic: 0.4° N). These sites are located in the auroral oval and in the EIA trough in the KISS network, respectively.

KIRN ROTI values in the aurora region were much higher than those at the CHUK site located in the EIA trough. This is not consistent with the results that equatorial GPS scintillations are generally more severe than those in high latitudes (Jiao & Morton, 2015). This may be due to the longitudinal distribution of ionospheric irregularities. It is noteworthy that GPS ROTI may reflect more phase scintillation rather than amplitude scintillation. CHUK ROTI values increased to ~0.5 TECU/min and ~1.1 TECU/min around LT=23:00 on March 16 and LT=21:30 on March 17, respectively. This may be explained by the climatological enhancement of the CHUK GPS TEC around LT=22:00 during spring (Chung et al. 2016). Most CHUK ROTI values higher

than 1.0 TECU/min were distributed at UT=09:30 (LT=19:30). This may be due to severe ionospheric irregularities caused by the increased PRE for geomagnetic disturbances. CHUK ROTI showed two small peaks of ~0.5 TECU/min and ~0.3 TECU/min near UT=15:00 (LT=01:00) and UT=18:00 (LT=04:00) at the second main phase and Kp=8. The variation in KIRN ROTI is similar to the AE index variation. The highest KIRN ROTI value was observed at geomagnetic latitude=63.3° and MLT=15:40 on March 17, 2015. This corresponds to the aurora oval with intense ROTI distribution (Cherniak & Zakharenkova 2016).

We conclude that GPS ROTI values from the KISS network can well represent ionospheric irregularities by geomagnetic disturbances in low and high latitudes. We expect that the routine GPS ROTI measurements can provide more opportunities to understand ionospheric dynamical responses to geomagnetic and atmospheric disturbances.

ACKNOWLEDGMENTS

REFERENCES

Aarons, J, Global morphology of ionospheric scintillations, Proc. IEEE 70, 360-378 (1982). https://doi.org/10.1109/PROC.1982.12314

Aarons J, Global positioning system phase fluctuations at auroral latitudes, J. Geophys. Res. 102, 17219-17231 (1997). https://doi.org/10.1029/97JA01118

Abadi P, Saito S, Srigutomo W, Low-latitude scintillation occurrences around the equatorial anomaly crest over Indonesia, Ann. Geophys. 32, 7-17 (2014). https://doi.org/10.5194/angeo-32-7-2014

Abadi P, Otsuka Y, Tsugawa T, Effects of pre-reversal enhancement of E×B drift on the latitudinal extension of plasma bubble in Southeast Asia, Earth Planets Space 67, 74 (2015). https://doi.org/10.1186/s40623-015-0246-7

Bang E, Lee J, Walter T, Lee J, Preliminary availability assessment to support single-frequency SBAS development in the

Korean region, GPS Solut. 20, 299-312 (2016). https://doi.org/10.1007/s10291-016-0522-4

Basu S, MacKenzie E, Basu S, Carlson HC, Hardy DA, et al., Coordinated measurements of low-energy electron precipitation and scintillations/TEC in the auroral oval, Radio Sci. 18, 1151-1165 (1983). https://doi.org/10.1029/RS018i006p01151

Cherniak I, Zakharenkova I, High-latitude ionospheric irregularities: difference between ground- and space-based GPS measurements during the 2015 St. Patrick's Day storm, Earth Planets Space 68, 136 (2016). https://doi.org/10.1186/s40623-016-0506-1

Cherniak I, Krankowski A, Zakharenkova I, Observation of the ionospheric irregularities over the Northern Hemisphere: methodology and service, Radio Sci. 49, 653-662 (2014). https://doi.org/10.1002/2014RS005433

Cherniak, I, Zakharenkova I, Redmon RJ, Dynamics of the high-latitude ionospheric irregularities during the 17 March 2015 St. Patrick's Day storm: ground-based GPS measurements, Space Weather, 13, 585-597 (2015). https://doi.org/10.1002/2015SW001237

Chu FD, Lee CC, Chen WS, Liu JY, A study of long-term climatology of ionospheric irregularities by using GPS phase fluctuations at the Brazilian longitudes, Adv. Space Res. 41, 645-649 (2008). https://doi.org/10.1016/j.asr.2007.05.003

Chung JK, Yoo SM, Lee W, The first measurement of seasonal trends in the equatorial ionospheric anomaly trough at the CHUK GNSS site during the solar maximum in 2014, J. Astron. Space Sci. 33, 287-293 (2016). https://doi.org/10.5140/JASS.2016.33.4.287

Deng B, Huang J, Liu W, Xu J, Huang L, GPS scintillation and TEC depletion near the northern crest of equatorial anomaly over South China, Adv. Space Res. 51, 356-365 (2013). https://doi.org/10.1016/j.asr.2012.09.008

Deshpande KB, Bust GS, Clauer CR, Kim H, Macon JE, et al., Initial GPS scintillation results from CASES receiver at South Pole, Antarctica, Radio Sci. 47, RS5009 (2012). https://doi.org/10.1029/2012RS005061

Jacobsen KS, Dähnn M, Statistics of ionospheric disturbances and their correlation with GNSS positioning errors at high latitudes, J. Space Weather Space Clim. 3, A27 (2014). https://doi.org/10.1051/swsc/2014024

Jacobsen KS, Andalsvik YL, Overview of the 2015 St. Patrick's day storm and its consequences for RTK and PPP positioning in Norway, J. Space Weather Space Clim. 6, A9 (2016). https://doi.org/10.1051/swsc/2016004

Jiao Y, Morton YT, Comparison of the effect of high-latitude and equatorial ionospheric scintillation on GPS signals during the maximum of solar cycle 24, Radio Sci. 50, 886-903 (2015). https://doi.org/10.1002/2015RS005719

Kintner PM, Kil H, Deehr C, Schuck P, Simultaneous total electron content and all-sky camera measurements of an auroral arc, J. Geophys. Res. 107, 1127 (2002) https://doi.org/10.1029/2001JA000110

Kintner PM, Ledvina BM, de Paula ER, GPS and ionospheric scintillation, Space Weather, 5, S09003 (2007). https://doi.org/10.1029/2006SW000260

Langley RB, the Integrity of GPS, GPS World, 60-63 (1999).

Li G, Ning B, Ren Z, Hu L, Statistics of GPS ionospheric scintillation and irregularities over polar regions at solar minimum, GPS Solut. (2010a). https://doi.org/10.1007/s10291-009-0156-x

Li G, Ning B, Hu L, Liu L, Yue X, et al., Longitudinal development of low-latitude ionospheric irregularities during the geomagnetic storms of July 2004, J. Geophys. Res. 115, A04304 (2010b). https://doi.org/10.1029/2009JA014830

Magdaleno S, Herraiz M, Altadill D, de la Morena BA, Climatology characterization of equatorial plasma bubbles using GPS data, J. Space Weather Space Clim. 7, A3 (2017). https://doi.org/10.1051/swsc/2016039

Muella MTAH, de Paula ER, Kantor IJ, Batista IS, Sobral JHA, et al., GPS L-band scintillations and ionospheric irregularity zonal drifts inferred at equatorial and low-latitude regions, J. Atmos. Sol.-Terr. Phys. 70, 1261-1272 (2008). https://doi.org/10.1016/j.jastp.2008.03.013

O'Hanlon BW, Psiaki ML, Powell S, Bhatti JA, Humphreys TE, et al., CASES: A smart, compact, GPS software receiver for space weather monitoring, Proceedings of the 24th International Technical Meeting of the Satellite Division of the Institute of Navigation, Portland, OR, 20-23 September 2011.

Pi X, Mannucci AJ, Lindqwister UJ, Ho CM, Monitoring of global ionospheric irregularities using the worldwide GPS network, Geophys. Res. Lett. 24, 2283-2286 (1997). https://doi.org/10.1029/97GL02273

Skone SH, The impact of magnetic storms on GPS receiver performance, J. Geodesy 75, 457-468 (2001). https://doi.org/10.1007/s001900100198